UDC 548.0; 535

ANISOTROPIC DISPLACEMENT PARAMETERS AND α-β PHASE TRANSITION IN QUARTZ-TYPE $FEPO_4$

M. Smirnov[1], N.A.Mazhenov[2] , N. Aliouane[3], P. Saint-Gregoire [(4,5)]

[1]Fock Institute of Physics, Physical Department of Saint-Petersburg State University, Petrodvoretz, 194508 St.-Petersburg, Russia
[2]Karaganda State Technical University, 100027 Karaganda, Kazakhstan
[3]Physics Department, Institute for Energy Technology, P.O. Box 40, NO-2027 Kjeller Norway
[4]University of Nimes, Dept Sciences and Arts, 30021 NIMES cedex, France
[5]University Montpellier 2, 34095 MONTPELLIER cedex, France

We present novel results on the mechanism of the a-b structural phase transition (STP) occurring in $FePO_4$. High accuracy X-ray diffraction experiments followed by a structural analysis, allow to get precise information on the thermal disorder change on different atomic sites. The data are analyzed at the light of lattice dynamics simulation results. The rigid unit mode (RUM) approach of the dynamics simulation allows the understanding of the anisotropic displacement parameters (ADPs). Surprisingly, the role of critical fluctuations of the order parameter, in the sense of Landau and Lifshitz theory, appears not relevant in the case of this SPT and the understanding of the dynamics requires the knowledge and analysis of the microscopic details of the system.

Keywords: Crystal, lattice, vibration, phonon, heat parameters

1. Introduction

The iron phosphate $FePO_4$ belongs to family of the ABO_4 compounds (A= Si, Ge, Al, Fe, Ga; B= Si, Ge, P, As) crystallizing in quartz-like structure. Within this family, only quartz, berlinite ($AlPO_4$) and iron phosphate undergo the high-temperature α–β phase transition [1-5]. This structural phase transition (SPT) has attracted much attention because of related anomalies in thermal expansion, elastic and optic properties [6]. The α–β SPT in $FePO_4$ stands out for its relatively high T_c value and for the highest volume increase. Recent renewal of the interest to the α–β SPT in $FePO_4$ was inspired by discovering of a new incommensurate phase [7-8] responsible for the small angle light-scattering anomalies [9-14]. The incommensurate state, intermediate between α- and β-phases, exists in $FePO_4$ within the temperature interval of 17 K [15], that is much wider than in quartz (1.5 K) [16-17] and in berlinite (2.5 K) [18-19].

Tracing the structure variation during the α–β SPT is of crucial importance for understanding the microscopic mechanism of the transformation. Considerable study has been given to anisotropic displacement parameters (ADPs) and to probability density functions (PDFs) in quartz and berlinite. It was found [20] that in quartz the ADPs for oxygen and silicon atoms in the directions closely related to the atomic displacements at the α–β transition show anomalous temperature dependence: at approaching critical temperature from bellow, they sharply (almost spontaneously) increase by about 30%, afterwards they decrease immediately after the transition. Besides, it was shown that the PDF for oxygen is eventually unimodal at all temperatures, but deviates considerably from Gaussian distribution in β-phase.

Origin of the non-Gaussian shape of PDF distribution in β-phase was confirmed by the results of molecular dynamics (MD) simulations [21]. It was discovered that the β-quartz structure, as it appears within MD simulation, has a peculiar dynamical character. When averaged over a long time, the probability distribution mimics a displacive shift to the ordered β-structure. However, analysis of the atomic trajectories shows that atoms hop between the two equivalent α1 and α2 structures by anharmonic motions with a temperature-dependent correlation time. Thus, the non-Gaussian PDF distribution for

β-phase matches well with superposition of two Gaussian distributions centered at α1 and α2 structures.

Experimental study of berlinite [22] did not revealed any remarkable differences as compared with quartz. The temperature dependencies of the positional and atomic displacement parameters were found strikingly similar to those of the corresponding atoms in quartz. The thermal ellipsoids for Al and P are oriented with their largest axes parallel to the two-fold axes at all temperatures. The Al–O and P–O bond distances are nearly constant in temperature. The highly anisotropic mean square displacements of O atoms were found to increase markedly with increasing temperature, especially in a narrow interval just below the critical point, in the directions nearly perpendicular to the librating Al-O-P bonds. Similarity of SPTs in quartz and berlinite was reinforced by results of MD study [23] which revealed the same double-Gaussian shape of PDF distributions for all atoms in the β-phase of berlinite.

A new look at the phase transition mechanism in quartz was reported in [24].The data obtained by using neutron total diffraction experiments and the Reverse Monte Carlo method clearly showed that the structure of the high-temperature phase does not consist of domains of an ordered structure, and does not involve the SiO_4 tetrahedra jumping between two orientations as in a classical order-disorder phase transition. The picture that emerged from Ref [24] showed that there is much more thermally-induced dynamic disorder than in either the classical soft-mode or the multi-domain models, and this disorder sets in at temperatures considerably below T_c. The important finding was that this considerable dynamic disorder is due not to the fluctuations of the order parameter *per se*, as in critical fluctuations, but to the excitation of new low-energy vibrations that are allowed to be excited as a result of the symmetry change associated with the phase transition.

From this result it can be suggested that the shape of PDF distribution in *β*–phase is not necessary dictated by the order-parameter fluctuation. Such a situation may occur at SPT in $FePO_4$, which structural characteristics were much lesser studied. The neutron diffraction study [5] revealed that behavior of this crystal during the α-β transformation is distinct from those of other quartz homologue in that the temperature-induced structural variations are much greater and do not scale with the initial β-to-α distortion. Important discontinuities in the structural parameters and atomic thermal amplitudes were observed in $FePO_4$ at the critical point. In author's opinion, this may be indicative of an essentially dynamic and the first-order character of this transformation. More cogent argument in favor of this idea could be obtained from analysis of ADPs.

The ADPs for $FePO_4$ were determined only for the room-temperature α-phase [2]. To our knowledge, no ADPs for β-$FePO_4$ were reported up to now. Only isotropic displacement parameters (IDP) were determined in the recent neutron diffraction (ND) study [5]. This paper reports refinement of structural parameters and ADPs for $FePO_4$ in α and β-phases obtained from analysis of X-ray synchrotron diffraction powder diagrams. The ADPs determined for β-$FePO_4$ differ significantly from those observed in quartz and berlinite. In order to clarify this difference, we performed lattice dynamics simulations, which allowed us to reveal the most unstable phonon modes determining ADPs in β-$FePO_4$ and to explain the particularity of this compound in framework of the model proposed in Ref [24].

2. EXPERIMENTAL RESULTS AND DISCUSSION

Anhydrous $FePO_4$ was prepared from commercial (Aldrich) powder of $FePO_4$, $2H_2O$ by annealing at about 670 K during 3 hours and at 720 K during 6 hours, which corresponds to optimal characteristics of the final powder (good crystallization and no parasite phase). The powder was then introduced in a silica capillary of 0.3 mm diameter. The X-ray diffraction pattern was collected at 1073 K (i.e. about 90 K above the phase transition temperature to avoid the α-phase coexistence) using a synchrotron source (Dw 22 line at LURE, λ=0.6883 Å in 2θ scan with a rotating sample. The temperature stability was better than 0.5 K. A diffraction pattern was also recorded at room

temperature in order to refine the structure of α-phase. We used the standard scattering lengths for Fe^{3+}, P^{+5} and O^{2-} ions. The intensities were corrected for linear absorption with μ=50.18 cm^{-1} and for the Lorentz and polarization effects. Among 290 reflections, 60 reflections in the 2θ range between 5 and 45º with I/sigma(I)>2 were used for the refinement of the β-structure.

For α-phase, we have started structure refinement with the atomic positions and ADPs borrowed from berlinite [4]. Finally, the α-$FePO_4$ structure was refined with reliability factor R_p = 4.9%. The X-ray diffraction diagram, collected at $T = 1073$ K, showed some peaks which could not be attributed within the symmetry group of β-$FePO_4$. Similarly, they could not be assigned to admixture of the orthorhombic $FePO_4$ structure, another allotropic form of iron phosphate [25]. Thus, we concluded that a parasite phase probably appears as a result of atomic diffusion into the $FePO_4$ sample from silica capillary tube. The determination of the space group and cell parameters of this parasite structure was performed by using the profile matching mode with a constant scale factor. This was done by using the X-ray reflections in the intervals in which there is no reflection from the $FePO_4$ itself. This led us to conclusion that the parasite structure belongs to space group *Pmmm* with unit cell parameters $a = 17.444$ Å, $b = 9.558$ Å, $c = 8.436$ Å and reduced the total reliability factor $R_p = 6.5\%$.

Thus determined structural parameters of both alpha and β-$FePO_4$ are shown in Table 1 in comparison with the results reported in Ref. [5]. All structural parameters of α-phase determined by both experimental techniques are close each other. The same is true for the positional parameters in β-phase. The unit cell parameters of β-phase lattice determined in our XRD study are slightly higher than those determined in [5].

Table 1. Unit cell parameters (in Å), fractional atomic coordinates and isotropic displacement parameters (in 10^{-2} $Å^2$) for α and β-phase structures of $FePO_4$

		α-phase[a], T=300K		**β-phase[b], T=1073K**	
		XRD, this work	ND, [5]	XRD, this work	ND, [5]
a		5.0287(9)	5.0314(1)	5.1907(8)	5.1621(4)
c		11.2291(0)	11.2465(2)	11.4320(8))	11.366(1)
Fe	*x*	0.4568(1)	0.4564(3)		
	U_{iso}	**1.00(2)**	0.79(3)	**3.16(3)**	3.1(2)
P	*x*	0.4595(3)	0.4545(6)	0.5	0.5
	U_{iso}	**1.05(2)**	1.01(4)	**7.28(5)**	5.3(4)
O1	*x*	0.4130(1)	0.4158(5)	0.421(4)	0.425(1)
	y	0.3121(9)	0.3195(4)	0.217(8)	0.222(3)
	z	0.3967(4)	0.3960(1)	0.589(3)	0.591(1)
	U_{iso}	**2.02(1)**	1.41(4)	**13.15(5)**	11.6(3)
O2	*x*	0.4113(8)	0.4099(5)		
	y	0.2673(7)	0.2621(4)		
	z	0.8738(1)	0.8760(1)		
	U_{iso}	**2.27(1)**	1.24(4)		
R_{Bragg}		0.024	0.022	0.053	0.26

a: Trigonal: P3121, Fe: 3a sites (x, 0, 1/3), P: 3b sites (x, 0, 5/6), O1 and O2: 6c sites (x, y, z)
b: Hexagonal: P6422, Fe: 3d sites (1/2, 0, 1/2), P: 3c sites (1/2, 0, 0), O: 12k sites (x, y, z)

Our structure refinement included determination of ADPs, which are defined as elements of the mean-square displacement matrix

$$U_{ij} = \left\langle \Delta x_i \Delta x_j \right\rangle .$$

The equivalent IDPs determined through U-matrix as

$$U_{iso} = \tfrac{1}{3}(U_{11} + U_{22} + U_{33}),$$

are presented in Table 1 in comparison with the values reported in Ref [5].

It is noticeable that the room-temperature U_{iso} values reported in [5] for α-$FePO_4$ are rather close to those reported for $AlPO_4$ [22]. The U_{iso} values obtained in our XRD study are systematically higher than those reported in Ref [5]. This excess is about 15% for all atoms in both α and β-phases with the exception of oxygen atoms in α-$FePO_4$ for which the excess runs to 65%. Besides, our results and the results of Ref [5] give different values for the ratio $U_{iso}(\mathrm{O1})/U_{iso}(\mathrm{O2})$: it is equal to 0.89 and 1.14, respectively.

In spite of these disagreements, the two experimental results show some coinciding trends which allow us to distinguish difference in behaviors of $FePO_4$ and $AlPO_4$. First of all, one should note that the increase of U_{iso} in course of the α-β transformation is much higher in $FePO_4$ than in $AlPO_4$. The data collected in Table 1 show that ratio of the U_{iso} values in β-phase and the room temperature α-phase in $FePO_4$ is about 5 for both cation atoms, whereas in $AlPO_4$ this ratio is 3.6 [22]. The same ratio for oxygen atoms is 4.7 in $AlPO_4$ [22], whereas for $FePO_4$ it is equal to 6 or 9, according to ND and XRD data respectively.

Consequently, all values of U_{iso} in β-$FePO_4$ are 1.6 -1.9 times higher than in β-$AlPO_4$. This difference cannot be explained by different temperatures of observation, because the U_{iso} values are almost temperature-independent in β-phases of both compounds [5, 22].

This is the first important distinction between two compounds.

Another noticeable difference between two compounds concerns the ratio $U_{iso}(\mathrm{A})/U_{iso}(\mathrm{B})$. In $AlPO_4$ it is close to unity at any temperature in both phases [22]. In $FePO_4$ this ratio is close to unity only in α-phase. In β-phase the ratio $U_{iso}(\mathrm{P})/U_{iso}(\mathrm{Fe})$ increases and runs to 2. This finding distinguishes $FePO_4$ from other quartz-type homologues, for which the relation $U_{iso}(\mathrm{A}) \approx U_{iso}(\mathrm{B})$ was suggested as a family property and was explained by strong A-O and B–O bonding in the two kinds of tetrahedrons, that makes the effects of the different masses less important in the librations [22]. It should be also mentioned remarkable difference between $AlPO_4$ and $FePO_4$ in variation of bond lengths. When comparing the bond lengths for the room-temperature α-phase structure and for the β-phase structure just after SPT, one can see that, according to ref [22], both Al-O and P-O bonds shorten by 2 and 8 percents respectively. According to our data, the Fe-O bonds shorten in SPT by 7 percent and the P-O bonds *lengthen* in SPT by 3 percent respectively. The same conclusion (even if with lesser difference between Fe-O and P-O bonds) can be drawn from the data reported in Ref [5].

A deeper insight into disorder nature of β-$FePO_4$ can be gained in analyzing the ADPs. It is convenient to characterize anisotropy of atomic displacements by lengths of the probability ellipsoid axes, the so-called Root Mean Square Displacements (RMSD), which are defined as square roots of eigenvalues of the U-matrix. In quartz-like ABO_4 structures, orientations of principal axes of the probability ellipsoids for A and B atoms are fixed by symmetry: one of them is directed along the two-fold axis C2, another one – along the three-fold axis C3, and the third one –

along C1 which is perpendicular to C2 and C3. We denote corresponding RMSD as R2, R3 and R1 respectively. The parameters for iron and phosphorus atoms derived from our experimental data are presented in Table 2 in comparison with analogous data for $AlPO_4$. It was found that R2 corresponds to the longest ellipsoid axis for A and B atoms in both phases of quartz [20] and berlinite [22]. Besides, R2 exhibits a sharp increase when passing the critical point. The R1 and R3 values both are lesser than R2, they are close each other and change smoothly during the SPT. The results presented Table 2 show that similar behavior is inherent to RMSDs of iron atoms in $FePO_4$. However, this is not the case for phosphorus atoms. According to our results, the longest ellipsoid axis for P atoms in both α and β-phases is R1 but not R2. Moreover, the R2 is the shortest ellipsoid axis for P atoms in β-$FePO_4$.

Table 2. RMSDs (in Å) for A and B atoms in two phases of $FePO_4$ and $AlPO_4$

$FePO_4$, this work			$AlPO_4$ [22]		
	α-phase T=300K	β-phase T=1076K		α-phase T=298K	β-phase T=904K
Fe R2	0.120(1)	0.237(8)	Al R2	0.0966	0.1975
R1	0.099(1)	0.118(1)	R1	0.0875	0.1583
R3	0.076(1)	0.157(8)	R3	0.0825	0.1567
P R2	0.103(1)	0.151(2)	P R2	0.0985	0.1831
R1	0.118(1)	0.328(4)	R1	0.0867	0.1640
R3	0.083(1)	0.256(1)	R3	0.0801	0.1692

Customarily, the probability ellipsoids of oxygen atoms in the quartz-like ABO_4 crystals are represented within the coordinate system attached to A-O-B angles. The three basis vectors are defined as follows. Vector n_2 is directed along bisector of the A-O-B angle, vector n_3 is perpendicular to the plane of the AOB angle, and n_1 is perpendicular to n_2 and n_3. In standard nomenclature used in vibrational spectroscopy, the oxygen atom oscillations along n_1 direction are referred as asymmetric A-O and B-O bond stretching. Normally, such vibrations are characterized by relatively high frequencies (~1000 cm^{-1}) and, hence, by low amplitudes. Oscillations along n_2 vector correspond to symmetric A-O and B-O bond stretching mixed with the AOB angle bending. Such vibrations are usually of relatively lower frequency (~400 cm^{-1}), and hence have higher amplitudes. The oscillations along n_3 direction correspond to rotations of the A-O-B bridge around A-B axis. They do not involve variations of 'rigid' internal coordinates - the bond lengths or AOB angle. Thus, they should have the lowest frequencies and the largest amplitudes. According to Refs [20, 22], these heuristic rules are perfectly fulfilled in quartz and berlinite: the ellipsoid axes of all O atoms, when listed in descending order, are oriented along n_3, n_2 and n_1 axes at all temperatures. According to our data, orientations of probability ellipsoids for O atoms in $FePO_4$ do not obey (or even partly contradict to) these rules. To describe quantitatively orientations of these ellipsoids, we introduced the coefficients $c_{ij} = (\mathbf{e}_i \mathbf{n}_j)$, here $\mathbf{e}_i$ is unit vector in direction of i-th ellipsoid axis. Taking into account that $\sum_j c_{ij}^2 = 1$, one can consider the quantity $100c_{ij}^2$ as a percentage of j-th direction in i-th ellipsoid axis. These coefficients for all oxygen probability ellipsoids are represented in Table 3.

One can see that in α-phase the shortest ellipsoid axes r3 for both O1 and O2 are directed presumably along $\mathbf{n}_1$ in good agreement with common rule. At the same time, the longest ellipsoid

axis r1 is directed presumably along $\mathbf{n}_2$ but not along $\mathbf{n}_3$, as it would be according to the common rule. According to our experimental data, the longest ellipsoid axis r1 for O atoms in β-$FePO_4$ is directed along $\mathbf{n}_1$ rather than along $\mathbf{n}_3$ as it takes place in quartz and berlinite, and the shortest one – presumably along $\mathbf{n}_2$ (not along $\mathbf{n}_1$ as it takes place in quartz and berlinite).

Table 3. Lengths and orientations of ADP ellipsoid axes for O atoms in α and β-$FePO_4$

	$100c_{ij}^2$				
	RMSD (Å)		n_1	n_2	n_3
O1 (α-phase)	r1	0.173(1)	0	99	0
	r2	0.153(2)	15	0	85
	r3	0.087(3)	84	1	15
O2 (α-phase)	r1	0.186(3)	24	58	18
	r2	0.170(1)	6	34	60
	r3	0.071(3)	70	8	22
O (β-phase)	r1	0.47(3)	89	11	0
	r2	0.31(2)	1	9	90
	r3	0.28(3)	12	78	10

It worth noting that, according to our results, the ADP ellipsoids of O atoms in $FePO_4$ have the form of lentils: lengths of two longer axes (r1 and r2) are close each other, and these axes are almost markedly longer than the shortest one (r3). This differs from results reported for quartz and berlinite, where the differences r1-r2 and r2-r3 were found almost equal at all temperatures. These results might indicate that the probability distribution for O atoms in β-$FePO_4$ is dictated not by atomic oscillations (this assumption is at the heart of the common rules), but rather by positional disorder related to complex multi-domain structure of this phase.

In order to verify this suggestion, we have refined structure of β-$FePO_4$ assuming the doubly split O positions. Thus we obtained two non-equivalent oxygen positions OI (0.416 0.260 0.565) and OII (0.427 0.196 0.615) with equal occupation numbers 0.5. These positions are spaced each other at 0.68 Å. Deviations of OI and OII from the O position obtained for the ordered β-phase structure are not equivalent. However, both vectors **x**(OI)-**x**(O) and **x**(OII)-**x**(O) are almost collinear with the O-displacements dictated by eigenvector of soft mode, i.e. they are almost parallel to **n**3. A fragment of the β-$FePO_4$ crystal structure with doubly split O positions is shown in Fig. 1. All previous studies of α-β transformation in quart-like ABO_4 crystals are agreed that the A-O-B bridges are conservative during the transformation. Guided by this notion, we have tried to develop a microscopic interpretation for the β-$FePO_4$ structure with the doubly split oxygen positions. Thus, two alternative interpretations were proposed. The first one, schematically depicted in Fig 1(a), assumes that the split configurations correspond to concordant rotations of all FeO_4 and PO_4 tetrahedra around C2 axes. This is just that is dictated by eigenvector of the classic soft-mode model. In this case, the P and Fe atoms displaced along the two-fold axes thus resulting in ATP ellipsoids mostly elongated is these directions. This is just the case of quartz and berlinite.

Another possible configuration, shown in Fig 1(b), implies that the split configurations come from rotations of FeO_4 tetrahedra around C2 axes accompanied by concordant rotations of PO_4 tetrahedra around C1 axes. Such distortion also can be accomplished without significant deformation of P-O-Fe bridges. In this case, the Fe and P atoms displace along the axes of tetrahedron rotations, i.e. along C2 and C1 axes respectively. This would result in different shapes of the ATP-ellipsoid for Fe and P atoms which would have the longest axis R2 and R1 respectively. This mechanism could explain our experimental results on ADPs.

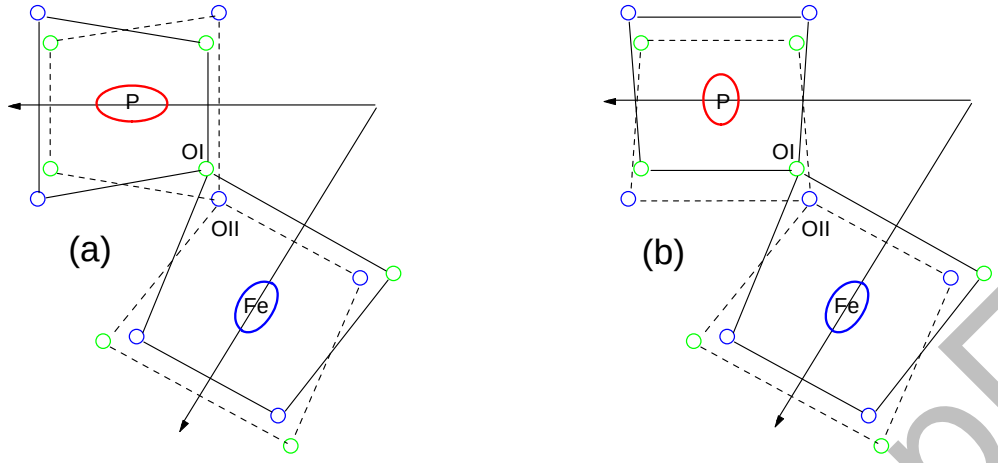

Fig. 1. Two possible arrangements of PO_4 and FeO_4 tetrahedra in β-$FePO_4$ structure with split O positions. The two-fold rotational axes are shown by arrows. Two equivalent tetrahedron orientations are shown by solid and dashed lines. Corresponding ATP ellipsoids of P and Fe atoms are shown by ellipses.

Both patterns of atomic displacements shown in Fig 1 involve tetrahedron rotations and translations. In order that they correspond to a phonon mode of low frequency, they must preserve integrity of the framework built up of the corner sharing tetrahedrons, tetrahedron deformation. From this condition it can be deduced that the atomic displacements motion shown in Fig. 1a must correspond to a zone-centre phonon mode, and that shown in Fig. 1b must belong to a zone-edge phonon mode with wave vector in the point A (0,0,1/2). Which of the two modes play more significant role in the lattice dynamics of β–phase depends on their relative stability?

3. LATTICE DYNAMICS ANALYSIS

In order to clarify this question, we performed lattice dynamics simulations and analyzed the whole set of the low-frequency phonon modes which must give the highest contributions to the atomic thermal amplitudes in β-$FePO_4$. Lattice dynamics α-$FePO_4$ was studied with the use of empiric potential model proposed by Mittal et al [26]. This potential model does not seem appropriate for our purposes because of two reasons. First, it predicts IADs of Fe atoms higher than those of P atoms at all temperatures [26]. This evidently contradicts to experimental observation. Second, it was built up with assuming transferability of the ionic charges and the P-O and the O-O pair-wise potentials between $AlPO_4$ and $FePO_4$. Thus, this model implies close similarity between the two compounds. This seems quite doubtful because electronic cloud of Fe^{3+} ion is an open-shell system with partially occupied *d*-orbitals. Consequently, the $[Al(OH)_4]^{1-}$ cluster used for evaluation of potential model parameters in $AlPO_4$ [27], is not appropriate for $FePO_4$. Indeed, the quantum-mechanical study of different clusters containing Fe-O-P bridges [28] and Al-O-P bridges [29] revealed essential difference in their electronic structures. In this connection, it is worth noting that high flexibility of the electronic structure of iron atoms connecting to phosphate groups manifests itself in large variability of their coordination numbers. This peculiarity hardly can be adequately taken into account in a simple potential model based on pair-wise interactions.

Such objective difficulties forced us to choose a simpler but more reliable approach. First of all, we analyzed the set of low-energy vibrations that are allowed to be excited in β-phase of $FePO_4$ as a result of the symmetry change induced by the phase transition, as it was suggested in Ref [24]. It was shown that that these low-frequency vibrations are closely related to Rigid Unit Modes (RUM) [30]. The RUMs are phonon modes in which the tetrahedra are able to move as rigid objects without distorting significantly, and hence RUMs give rise to the vibrations with the lowest

frequencies. Low frequencies lead to large amplitudes, and this means that the large amplitude rotations and displacements of the tetrahedra in the β-phase configuration are primarily due to the excitation of the modes coming from RUMs. Detailed calculations have shown that there are significantly more RUMs in the β-phase than in the *α*-phase, and this fact results from the symmetry change associated with the phase transition [30].

The whole set of RUM in b-quartz was analyzed in Ref. [30]. Here we recall only main results. If one assumes absolute rigidity of the SiO_4 tetrahedrons and neglects any long-range interactions, then it turns out that the phonon states of such lattice can be divided into two groups: ones involving the inter-tetrahedron deformations and having very high frequency and others (namely RUMs) with zero frequency. It was shown that RUMs are primarily located along symmetric lines in BZ. Their distribution within the BZ of a quartz-like lattice is schematically shown in Fig. 2.

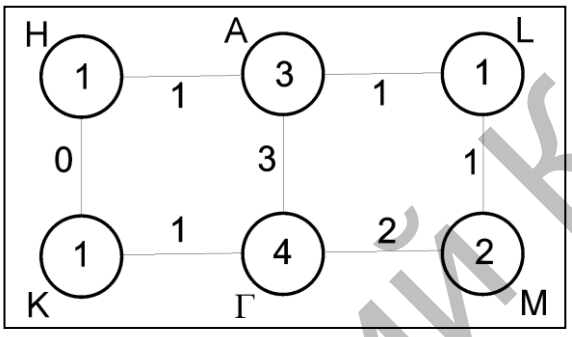

Fig 2. Distribution of RUMs in BZ of β-quartz

In order to understand in which manner different RUMs affect anisotropy of atomic thermal displacement one has to visualize shapes of the RUMs in symmetric point of BZ. They are shown in Fig. 3. We labeled every RUM by a letter, which indicates corresponding point within BZ, and by index which enumerate the RUM belonging to the same BZ points. Thus, we have one Γ-RUM (see Fig 3(a)), which plays a role of soft mode for the classic displacive a-b phase transition (cf. Figs 1a and 3a). Three other Γ-RUMs are conventional translations which give rise to three acoustic branches. Besides, we have three A-RUMs, two of them are twice degenerated. Non-degenerated A-RUM and one component of the doubly degenerated A-RUMs are shown in Figs 3b and 3c. In fact, all A-modes imply alteration of displacements of atoms translated along z-axes. This should be taken into account when considering Figs 3b and 3c in which the z-positions of tetrahedrons are given by small numbers. Finally, we have two M-RUMs and one K-RUM shown in Fig 3d-3f. One can see that these modes primarily consist of rotations of the tetrahedrons. The only exception concerns M1-mode (see Fig 3d) in which a half of the tetrahedrons execute pure translations.

It should be pointed out that in the some RUMs rotations of tetrahedrons are accompanied by their translations along directions of rotational axis. This peculiarity takes place in the Γ-RUM and A1-RUM and is due to condition of preservation of integrity of the framework. For these modes, one can roughly estimate directions of translations of tetrahedrons in the xy-plane by the long thin arrows indicating the rotational axes.

In this study, our particular interest is to reveal the modes which determine anisotropy of ADPs of the cation atoms (the centers of tetrahedrons) in the *xy*-plane. Thus, we focus our attention on three modes Γ-RUM, A1-RUM and M1-RUM which involve considerable amount of the tetrahedron translations in *xy*-plane. There are three M-points in BZ. Correspondingly, there are three M1-RUMs (similar to that shown in Fig. 3d) with translational motions along (100), (010) and (110) crystallographic directions. From this it follows that these modes do not contribute in anisotropy of ADP of the central atoms in the xy-plane.

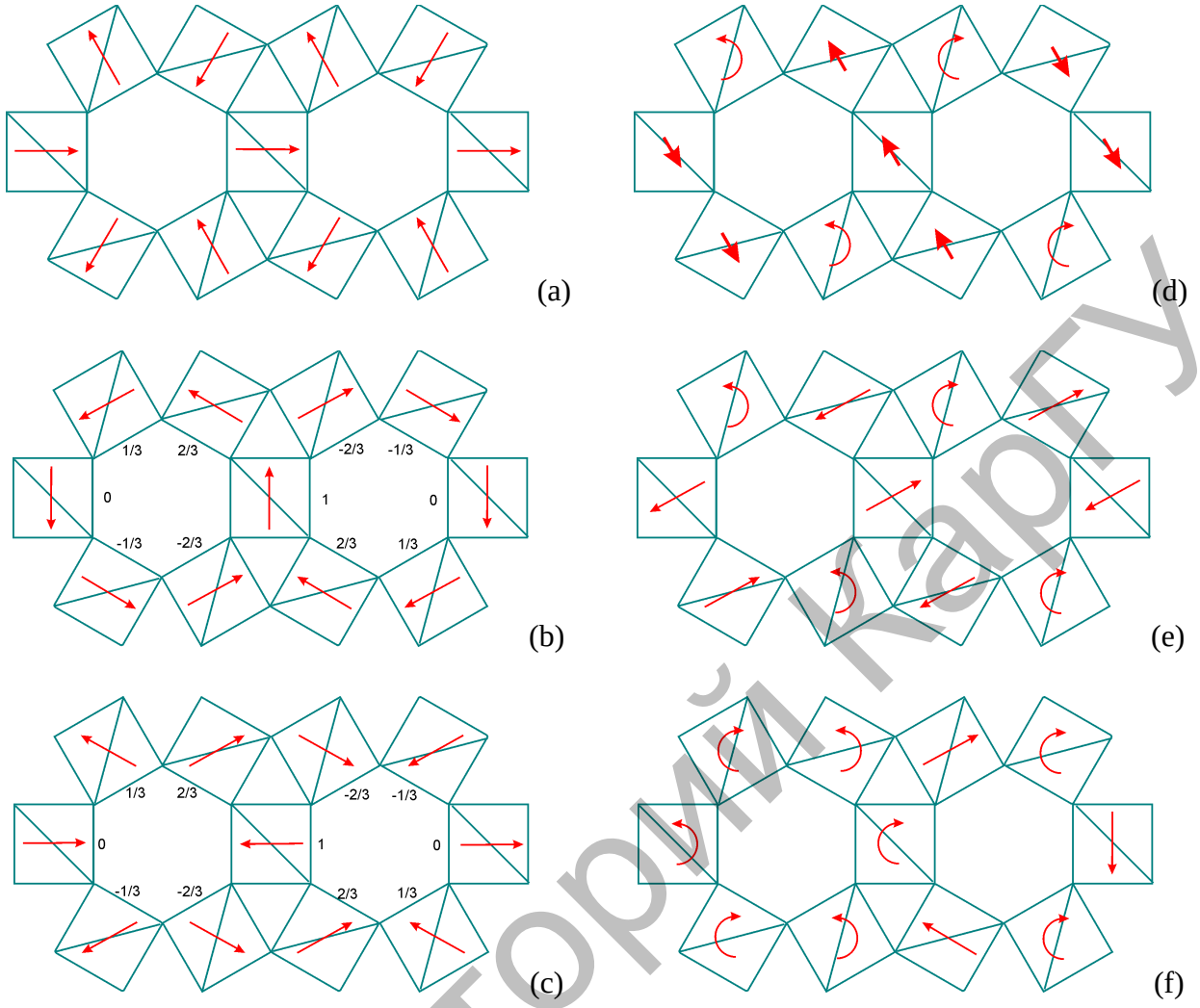

Fig 3. Shapes of different RUMs in b-quartz: Γ-RUM (a), A1-RUM (b), A23-RUM (c), M1-RUM (d), M2-RUM (e), and K-RUM (f). Curvy arrows show direction of rotation around axis parallel to *z*, long and thin arrows show direction of rotational axis lying in *xy*-plane, and thick arrows show translations of tetrahedrons in *xy*-plane. Small numbers in (b) and (c) indicate positions of tetrahedrons along *z*-axis.

Contrariwise, the Γ-RUM and A1-RUM evidently affect this anisotropy. The former mode involves the tetrahedron translations along the C2 axes, and the latter mode – in the perpendicular direction, i.e. they contribute to R2 and R1 values, respectively. Experimental studies of β-quartz [31] confirmed the soft-mode behavior for Γ-RUM, whereas no soft mode was found in A-point, as far as we know. This is in line with other experimental data [20] which estimate R2 markedly greater than R1.

This model works equally well for quartz and berlinite, even if another BZ direction (Γ-A) contains three times more RUMs. This phenomenon takes place because the Γ-RUM softens at approaching the critical point much more rapidly than other RUMs. This result is closely related to the condition that both AO_4 and BO_4 tetrahedrons are of about the same rigidity. This is not the case for $FePO_4$. In view of markedly longer Fe-O bonds, one can suggest that the FeO_4 tetrahedrons must be essentially softer than PO_4 tetrahedrons. This suggestion is confirmed by the fact that IDP of Fe and P atoms in a-phase are almost equal despite the great difference in mass. This particularity of $FePO_4$ may cause important changes in the low-frequency part of the phonon spectrum and, consequently, in the shape of ADP-ellipsoids in comparison with other quartz-like crystals. Below we advance some quantitative arguments in favor of this suggestion.

One can consider the berlinite-like ABO_4 lattice as that originated from a doubling of unit cell of the quartz-like AO_2 lattice in c-direction accompanied by alteration of atoms A and B in the neighboring cation positions. If the difference between A and B atoms is not significant, the phonon spectrum of the berlinite-like lattice can be represented as that resulted from folding of BZ of the quartz-like lattice with respect to (0 0 ¼) plane. In such a case, distribution of RUMs within BZ of the berlinite-like ABO_4 lattice can be represented by the schema similar to that shown in Fig. 2 with doubled number of RUMs along all special directions and points in BZ.

Due to folding of the BZ, the modes belonging to A-point in the quartz-like lattice transform into zone-centre modes in the berlinite-like lattice, and the phonons belonging to (0 0 ¼) point in the quartz-like lattice transform into A-phonons in the berlinite-like lattice. Thus, in G and A points of berlinite there are 7 and 6 RUMs, respectively. Among them only 4 RUMs have eigenvectors which exhibit clearly anisotropy of tetrahedron translations. Two of them come from the mode shown in Figs (a) and (b) (both of them belong to G-point in berlinite-like structure and shall be referred below as Γ1 and Γ2). And two other such RUMs originate from (0 0 ¼) phonons in quartz-like lattice and belong to A-point in the berlinite-like structure. They are of particular interest, because they involve atomic displacements which provide different anisotropy of ADP for A and B atoms. One of these modes is shown in Fig 4. It can be seen that in this modes all AO_4 tetrahedrons rotate around C2-axes and all BO_4 tetrahedrons rotate around C1-axes. For another 'twin' mode the situation is reciprocal – the BO_4 tetrahedrons rotate around C2-axes and the AO_4 tetrahedrons rotate around C1-axes. We shall refer these two modes as A(A) and A(B) modes. Recall that in both the modes the tetrahedrons accomplish translational motions along their axes of rotations.

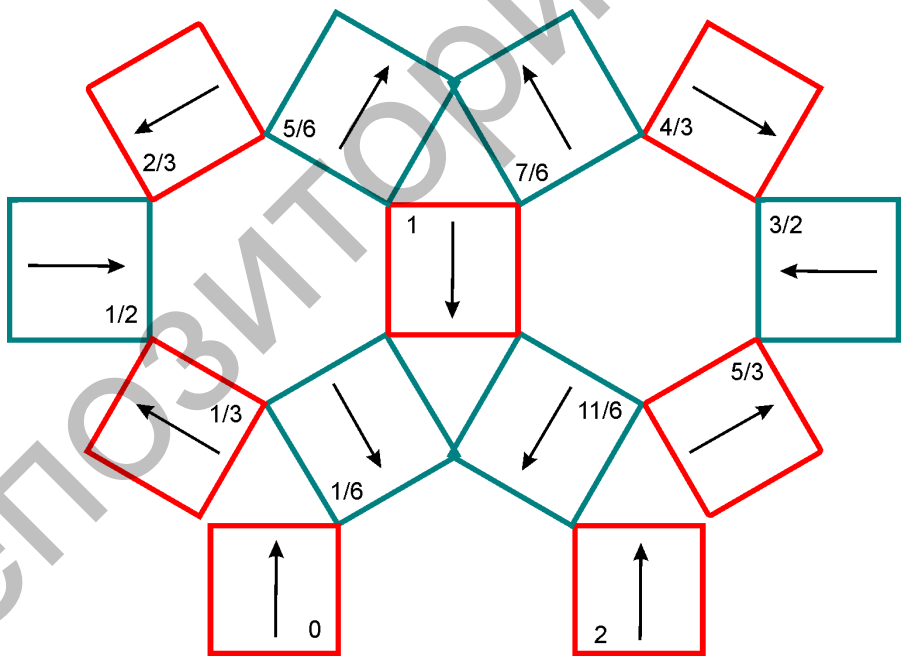

Fig 4. A fragment of β-ABO_4 structure in *xy*-projection. Contours AO_4 and BO_4 tetrahedrons are shown by blue and red squares. The z-positions of the tetrahedrons are given by small number. Arrows show orientations of rotational axes inherent to A(A)-RUM.

It should be emphasized that namely large amplitude of the A(A)-mode is the very essence of hypothesis, depicted in Fig 1b, which could provide explanation to anisotropy of ADPs observed in our experiments on $FePO_4$. In order to justify this hypothesis, we have to show that A(A)-RUM actually is one of the softest mode in β-$FePO_4$.

Strictly speaking, in a real crystal, in which tetrahedrons are deformable and the long-range interactions are not negligible, the low-frequency modes may somewhat differ from RUMs. In order to estimate relative contributions of different phonon modes in the thermal atomic amplitudes, we have simulated phonon spectrum of the ABO_4 crystals with the use of simple potential model, which takes into account the finite compressibility of the PO_4 and FeO_4 tetrahedrons and the middle-range O-O interaction. Thus, our dynamic matrix included two contributions. The first one, corresponding to the A-O and B-O bond stretching deformations, was derived from harmonic potential function

$$U = \tfrac{1}{2}\sum_n \sum_{i=1}^{4} K_n (R_{ni} - R_n^0)^2 \ ,$$

here R_{ni} is simultaneous length of the *i*-th bond in *n*-th tetrahedron, R_n^0 is the equilibrium value of the bond lengths, and K_n is corresponding force constants. Values of R_n^0 were chosen as lengths of the A-O and B-O bonds in the room-temperature a-structure. As the first approximation, the K_n value can be assumed equal for all homologous bonds. Thus, for every compounds it remains only two independent force constants for A-O and B-O bonds which we denote as K_A and K_B. Their values were chosen in such a way as to reproduce best the frequencies of two phonon modes which give rise to two the most intense Raman lines. One of them involves the anti-phase pulsations of the AO_4 and BO_4 tetrahedrons, and another one involves in-phase deformations of the A-O-B bridges. Hence, frequencies of both the modes are rather sensitive to the bond-stretching force constants.

The second term of dynamic matrix, that corresponding to interactions between *m*-th and *n*-th O atoms was described by Born's longitudinal pair-wise force constants $A_{mn} = \dfrac{\partial^2 U}{\partial r_{mn}^2}$, whose values were assumed to depend on O-O distance r_{mn} according to relation

$$A_{mn} = A_0 \exp\left(-\frac{r_{mn}}{\rho}\right)$$

Parameter $\rho = 0.375$ Å was chosen as the average of values used in potential models previously reported for the crystals under study [21, 23, 27]. Parameter $A_0 = 86000$ N/m was chosen so that the low-frequency parts of the phonon spectra of all the structures cover the interval between 100 and 400 cm^{-1} (in accordance with experimental data). It should be emphasized that in such a simple model there are only three fitting parameters K_A, K_B and A_0. Besides, the A_0 value was guessed the same for all compounds under study. Thus obtained model parameters are represented in Table 4 along with calculated frequencies which are compared with experimental data. Note that the values of force constants used in our model correlate with lengths of the bonds and are in line with the values used in more sophisticated valence force field models [32, 34].

Table 4. Model parameters and frequencies (in cm^{-1}) of some phonon modes.

ABO_4	R_A^0, R_B^0 (Å)	K_A, K_B (N/m)	ν1, ν2 (calc.)	ν1, ν2 (exp.)
SiO_2	1.609	360	1068, 469	1080, 464 [32]
$AlPO_4$	1.735, 1.523	320, 475	1107, 464	1112, 461 [33]
$FePO_4$	1.850, 1.542	180, 440	1015, 412	1015, 405 [Past]

Then we used the potential model to calculate phonon frequencies for the β-phase ABO_4 lattices. The structural parameters for β-quartz and β-berlinite were taken from experimental data [20, 22] and for β-FePO4 from Table 1. The phonon-states in the low-frequency part of spectrum are very sensitive to structure variations accompanying α-β transformation. First of all, this is due to kinematical reason mentioned above: some modes involving intra-tetrahedron deformations in a-phase become pure RUMs in β-phase. Second reason is related to the bond length variation. Both A-O and B-O bonds shorten markedly in the β-phase. This bond shortening induces intra-tetrahedral tensions which produce destabilizing effect on the modes involving rotations of the tetrahedrons [35]. As a consequence, many of such rotational modes become unstable in the harmonic approximations. This means that corresponding oscillations are not longer described by a single-minimum potential but a double-minimum potential well [36]. Namely these modes having imaginary values of harmonic frequencies mostly contribute to the thermal atomic amplitudes. The more is imaginary part of the frequency the higher is this contribution.

The calculated frequencies of RUMs of interest are shown in Table 5. It is seen that in β-quartz and β-berlinite all bonds become shorter that in α-phase. The bond reduction amounts to 0.047, 0.025 and 0.033 Å for Si-O, Al-O and P-O bonds, respectively. All these bonds are rather rigid as judged from the force constant values cited in Table 5. Therefore, shortening of these bonds induces significant internal tensions in all the tetrahedrons, and all the consider RUMs become harmonically unstable. In β–quartz, frequencies of A(A)-RUM and A(B)-RUM are identical by symmetry constraint. It is remarkable that these frequencies are almost equal in β-$AlPO_4$. So, these modes having similar amplitudes cannot lead to different anisotropy of ADPs for Al and P atoms. This anisotropy is determined by difference in frequency between Γ1-RUM and Γ2-RUM. The former is more unstable. This gives rise to ADP ellipsoids elongated along C2 axes for all heavy atoms in β-SiO_2 and β-$AlPO_4$.

Table 5. Bond lengths in β-phase ABO_4 structures and calculated frequencies (in cm^{-1}) of phonon modes related to RUMs

ABO_4	R_A, R_B (Å)	Γ1-RUM	Γ2-RUM	A(A)-RUM	A(B)-RUM
SiO_2	1.5624	83i	28i	82i	82i
$AlPO_4$	1.7091, 1.4902	58i	43	34i	38i
$FePO_4$	1.7128, 1.5850	38i	27	19i	22

The situation is different in the case of β-$FePO_4$ in which α-β transformation produces different changes for Fe-O and P-O bonds. According to our experimental data, the former bonds shorten by 0.138 Å and the latter bonds lengthen by 0.043 Å. Origin of this particularity cannot be explained in the framework of such a simple phenomenological model as ours. It is very likely that it is related to considerable difference in rigidity of Fe-O and P-O bonds. However, our model allows us to predict the impact of this particular feature on the low-frequency phonon states in β-$FePO_4$. First of all, the results of calculations show significant difference between A(A)-RUM and A(B)-RUM. The latter mode is harmonically stable. Contrariwise, the A(A)-RUM is unstable with imaginary frequency quite comparable with the frequency of the Γ□-RUM. Atomic displacements corresponding to this mode are shown in Fig 5. They are strikingly similar to the atomic displacements dictated by structural model with disordered O positions derived from our experimental data (cf. Figs. 1b and 5).

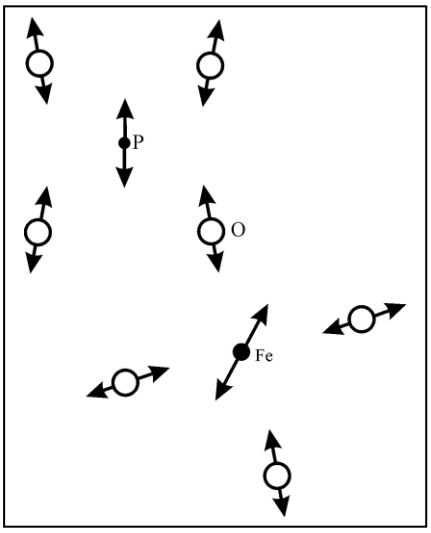

Fig 5. Directions and amplitudes of atomic oscillations within A(A)-RUM obtained from lattice dynamics simulations.

4. Conclusion

So, it should be pointed out that in the some RUMs rotations of tetrahedrons are accompanied by their translations along directions of rotational axis. This peculiarity takes place in the Γ-RUM and A1-RUM and is due to condition of preservation of integrity of the framework. For these modes, one can roughly estimate directions of translations of tetrahedrons in the xy-plane by the long thin arrows indicating the rotational axes.

This result of our calculations, based on a rather simple potential model, cannot be considered as a final verdict. Nevertheless, it provides some justification for our hypothesis and shed some light on the rather unusual experimental results showing significant difference in anisotropy of ADPs for Fe and P atoms in $FePO_4$.

REFERENCES

1. H. Grimm and B. Dorner, J. Phys. Chem. Solids. 36, 407 (1975).
2. H. Ng and C. Calvo, Can. J. Phys. 54, 638 (1976).
3. K. Kosten and H. Arnold, Zeistschrift fur Kristallogr. 152, 119 (1980).
4. A. Goiffon, J. C. Jumas and E. Philippot, Revue de Chiime Minerale 23, 99 (1986).
5. J. Haines, O. Cambon and S. Hull, Z. Kristallogr. 218, 193 (2003)
6. G. Dolino, Phase Transitions 21, 59 (1981).
7. T.A. Aslanyan, T. Shigenari and K. Abe, J.Phys. Cond. Matter 10, 4577 (1998).
8. P. Saint-Gregoire, E. Snoeck and N. Aliouane, Ferroelectrics 252, 1 (2001).
9. I. A. Yakovlev , L. F. Mikheeva and T. S. Velichkina, Sov. Phys. Cryst. 1, 91 (1956).
10. S. M. Shapiro and. H. Z Cummins, Phys. Rev. Lett. 21, 1578 (1968).
11. G. Dolino, Phys. Stat. Solidi (a), 60, 391 (1980).
12. H. Z. Cummins and A. P. Levanyuk, *Light Scattering near Phase transitions,* (North-Holland Publising Compagny, 1983), p. 605.
13. G. Dolino, F. Mogeon and V. Soula, Phase Transition 36, 129, (1991).
14. P. Saint-Gregoire et al., JETP Letters 64, 376 (1996).
15. N. Aliouane et al., Ferroelectrics 241, 255 (2000).
16. G. Dolino, J. P. Bachheimer and C.Zeyen, Solid State Commun. 45, 295 (1983).
17. K. Gouhara, Y. H. Li and N. Kato, J. Phys. Soc. Japan 52, 3697 (1983).
18. J. P. Bachheimer et al., Solid State Commun. 51, 55 (1984).
19. J. Durand, M. Lopez, L. Cot and P. Saint-Gregoire, J. Phys. C. : Solid State Phys. 16, 3\\ (\983).
20. K. Kihara. Eur. J. Mineral. 2, 63 (\990)
21. S. Tsuneyuki, H. Aoki, and M. Tsukada, Phys. Rev. Lett. 64, 778 (\990)

22. Y. Muraoka and K. Kihara, Phys. Chem. Minerals 24, 243 (\997)
23. K. Kihara and M. Matsui, Phys. Chem. Minerals 26, 60\ (\999)
24. M. G. Tucker, M. T. Dove and D. A. Keen, J. Phys. Condens. Matter 12, L723 (2000)
25. J. Rodriguez-Carvajal, Physica B 192, 55 (\993), see also : *Recent Developments of the Program FULLPROF, in Commission on Powder Diffraction* (IUCr). Newsletter (200\), 26, \2-\9. (http://iournals.iucr.org/iucr-top/comm/cpd/Newsletters/)
26. W. Eventoff, R. Martin, and D. R. Peacor, Am. Mineralogist 57, 45 (\972).
27. R. Mittal, S. L. Chaplot, A. I. Kolesnikov, C.-K. Loong, O. D. Jayakumar, and S. K. Kulshreshtha, Phys. Rev. B 66, \74304 (2002).
28. G. J. Kramer, N. P. Farragher, B. W. H. van Beest, and R. A. Santen, Phys. Rev. B 43, 5068 (\99\)
29. A. Dhouib, C. Minot, M. Abderrab, J. Molec. Struc. THEOCHEM 860, \6\ (2008).
30. I. S. Ignatyev, T. Sundius, J. Molec. Struc. THEOCHEM 480-481, 667 (\999).
31. K. D. Hammonds, M. Dove, A. P. Giddy, V. Heine, and B. Winkler, Amer. Mineralogist, 81, \057 (\996).
32. M. B. Smirnov, Phys. Rev. B 59, 4036 (\999).
33. Y. Tezuka, S. Shin, and M. Ishigame, Phys. Rev. Lett. 66, 2356 (\99\)
34. M. P. Pasternak, G. Kh. Rozenberg, A. P. Milner, M. Amanowicz, T. Zhou, U. Schwarz, K. Syassen, R. Dean Taylor, M. Hanfland, and K. Brister, Phys. Rev. Lett. 79, 4409 (\997).
35. A. P. Mirgorodskii, Opt. Spektrosk 48, \83 (\980)
36. I. Gregora, N. Magneron, P. Simon, Y. Luspin, N. Raimboux, and E. Philippot, J. Phys. Condens. Matter 15, 4487 (2003)
37. N. A. Mazhenov, M. B. Smirnov and B. F. Shchegolev, Opt. Spektrosk. 72, \29 (\992)
38. P. Mirgorodsky and M. B. Smirnov, Ferroelectrics, 159, \33 (\994).

Article accepted for publication 3.09.2012